

Supporting Information for "Local hydraulic conductivity in heterogeneous porous media"

Quirine Krol¹, Itzhak Fouxon^{1,2}, Pascal Corso¹, Markus Holzner^{1,2,3,4}

¹ETH Zurich, Stefano Franscini-Platz 5, 8093 Zurich, Switzerland

²Department of Computational Science and Engineering, Yonsei University, Seoul 120-749, South Korea

³Swiss Federal Institute for Water Science and Technology EAWAG

⁴Swiss Federal Institute for Forest, Snow and Landscape Research WSL

Contents of this file

1. Direct numerical simulation of Stokes flow in porous media.
2. Pseudo code: Measuring local hydraulic conductivity.
3. Measuring the Transversal and Longitudinal Energy Dissipation tensor.

Additional Supporting Information (Files uploaded separately)

1. Isopressure surfaces video
2. Pore identification video

Introduction

Below we describe the necessary steps and specific settings of the analysis presented in methodology. The first part consists of the description of the direct numerical simulations performed that are used as a numerical experiment. In the second part we describe the

details of the extraction of iso pressure surfaces and fluxes from which the hydraulic conductivity is calculated and integrated along consecutive pores. In the last part we take three samples from the three porous media to test the hypothesis that is made in Eq.() of the main article.

Direct Numerical Simulations To generate heterogeneous porous media we have used Gaussian Random Fields to generate 3 porous media. A threshold is used to define the porous media-fluid interface Γ and its porosity. eq 0.6, .5 and .25. These porous media are used as input for direct numerical simulations (OpenFOAM v. 4.1) Weller, Tabor, Jasak, and Fureby (1998) that solves the Navier-Stokes equations in the pore space. The boundary conditions are defined at the inlet p_1 and outlet p_2 and a no-slip for the porous media-fluid interface. A visualization of the three porous media an the result of the DNS is visualized in Fig. ??

- Three geometries generated by gaussian random fields, with porosity, specific surface area, Euler characteristic of
- DNS employed with boundary conditions at the inlet and outlet defined by δp . A no slip boundary condition is enforced on the domain walls as well as the porous media interface.

- Result of the DNS gives estimated Re numbers by

$$Re = u/s\eta \quad (1)$$

- Residuals were standard, check 10^{-6} took about 8 hours using 32 cores using the Euler cluster.

Extraction of pores based on isopressure surfaces Then a chain of VTK-based image analysis techniques Schroeder, Martin, and Lorensen (2006); Hernderson (2007) are employed to extract iso-pressure surfaces $\mathcal{S}(p)$ and enumerate the disconnected areas identifying as an iso-pressure slice $\mathcal{S}_i(p)$, part of a pore and measure its surface area $A_i(p)$, sphericity $\gamma_i(p)$, average location $\mathbf{x}_i(p)$ and average flux $Q_i(p)$. For each $\mathcal{S}_i(p)$ its closest neighbor $\mathcal{S}_j(p + \delta p)$ is identified by its smallest distance $d_{i,j} = |\mathbf{x}_i(p) - \mathbf{x}_j(p + \delta p)|$. By forward integration of the first iso-pressure patches $\mathcal{S}_i(p_0)$ we identify all patches belonging to the same pore $\mathcal{P}_l(\Delta p) = \{\mathcal{S}_k(p_i)\}$. By conditioning the distances of consecutive iso pressure patches to a maximum, the ends of a pore is defined. When a splitting/merging of pores is at hand, the average position is rather sensitive, and the distance between two consecutive iso-pressure pore patches will exceed the maximum distance. Fig. ?? shows a visualization of the positions of the identified pores. For each δp we can now evaluate Eq. ?? and for each pore, we can evaluate Eq. ?. A visualization of an iso-pressure surface $\mathcal{S}(p)$ and its deviation of patches is shown in Fig.??.

Measuring the relative Longitudinal and Transversal energy dissipation on an isopressure surface In the theoretical section of the paper we have derived expressions for the longitudinal and transversal energy dissipation tensors, by

$$|\nabla_i u_j|^2 \approx |\nabla_s u_p|^2 + |\nabla_n u_p|^2. \quad (2)$$

where we have assumed that the terms $|\nabla_n u_n|^2$ and $|\nabla_s u_n|^2$ are negligible. We will show two examples where we have calculated the individual terms of the total viscous dissipation. Because the highest dissipation is expected to be located near the porous media interface and the discretization also refined at the interface the numerical noise is also expected to be higher, see FigS1. All 3 porous media contain some points in the mesh

where the VTK gradient filter can't factorize the linear system which leads to very high values of the respected fields. The origin lies likely in the mesh quality generated by the snappyHexMesh generator contained in the openFoam simulation. Since the simulations have all converged we do not question the original simulation results but we do note that post-processing of these meshes can be difficult especially if gradients have to be calculated. Nevertheless we have tried to quantify the relevance of the transversal and longitudinal terms of the viscous dissipation tensor. We have chosen to threshold the unreasonable high gradient terms based on outliers in the histograms of the gradients. For the first porous media the porous media the refinement was chosen a degree higher than the others, and led to 'nan' results of the integrated relative contributions. For the two other porous media we have found reasonable results given in Table . Since we have to filter out quit some data that exhibits unreasonable high values the percentages are not adding up to 100%. By visual inspection we can examine the term $|\nabla_i u_j|^2$ in all porous media and we see that the total dissipation correlates with gradients in the transverse direction. Also in this data we can see that for Porous Media 3 the relative contribution of the longitudinal term $|\nabla_n u_p|^2$, 24% is in the same order as the transversal term $|\nabla_s u_p|^2$ which amounts to 32%. This observation is in agreement with the fitting of the two contributions in the paper.

PM	$ \nabla_s u_p ^2$	$ \nabla_n u_p ^2$	$ \nabla_n u_n ^2$	$ \nabla_s u_n ^2$
PM2	71%	17%	12%	12%
PM3	32%	24%	10%	5%

Table S1. Estimated relative contributions to the total viscous dissipation on an iso-pressure surface.

References

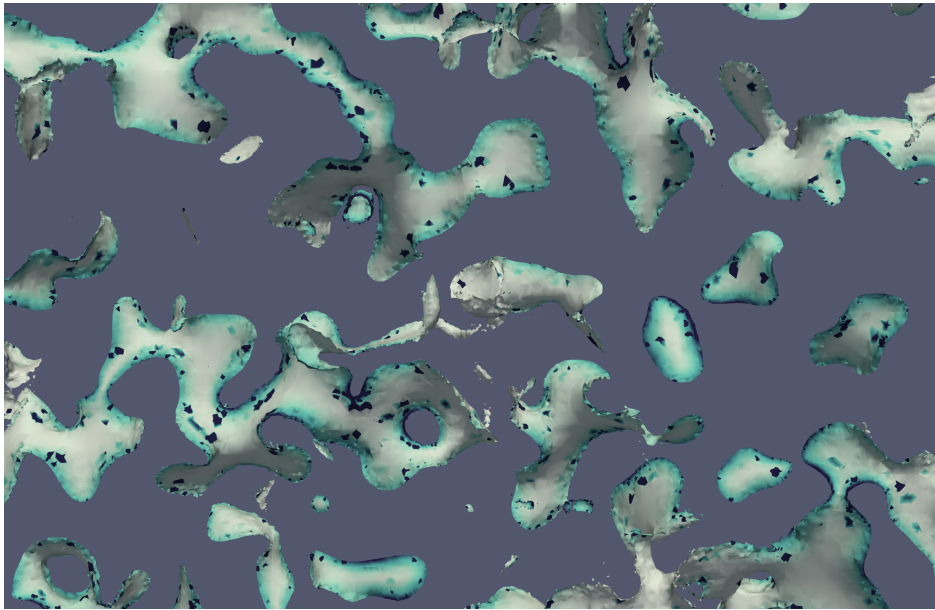


Figure S1. A visualization of the energy dissipation tensor $|\nabla \otimes \mathbf{u}|$ on a iso-pressure surface of PM1, indicating the numerical issues

Hernderson, A. (2007). *ParaView Guide, A Parallel Visualization Application*.

Schroeder, W., Martin, K., & Lorensen, B. (2006). *The visualization toolkit: An object-oriented approach to 3D graphics ; [visualize data in 3D - medical, engineering or scientific ; build your own applications with C++, Tcl, Java or Python ; includes source code for VTK (supports Unix, Windows and Mac)* (4. ed ed.). Clifton Park, NY: Kitware, Inc.

Weller, H. G., Tabor, G., Jasak, H., & Fureby, C. (1998, December). A tensorial approach to computational continuum mechanics using object-oriented techniques. *Computers in Physics*, 12(6), 620. doi: 10.1063/1.168744